

Stomatal conductance changes due to increasing carbon dioxide levels: Projected impact on surface ozone levels

By M. G. SANDERSON*, W. J. COLLINS, D. L. HEMMING and R. A. BETTS, *Hadley Centre,
Met Office, Fitzroy Road, Exeter, EX1 3PB, UK*

(Manuscript received 28 April 2006; in final form 23 January 2007)

ABSTRACT

The impact of increasing levels of carbon dioxide on stomatal conductance and surface ozone levels was investigated using a global three-dimensional general circulation model (GCM) coupled to an interactive land surface scheme and a chemistry model. Pre-industrial, present day and doubled present day levels of carbon dioxide were used. This approach was used to examine the sensitivity of modelled surface ozone levels to changes in stomatal conductance via dry deposition. A doubled level of carbon dioxide was found to increase surface ozone levels by between 2 and 8 ppb in all four seasons owing to reduced dry deposition fluxes, although the location and extent of the changes were very different between each season. No change in levels of nitrogen oxides (NO and NO₂) was modelled. A similar experiment to examine the same effect on modelled pre-industrial ozone levels showed that the ozone levels over Europe were only slightly smaller (by 1–1.5 ppb) when the CO₂ level was decreased from 369 ppm to 280 ppm.

1. Introduction

The levels of carbon dioxide (CO₂) in the atmosphere have increased over the last 150 years, from about 280 ppm in the pre-industrial era to 369 ppm in the year 2000 (IPCC, 2001). This increase in carbon dioxide levels is caused mostly by the burning of fossil fuels, with a smaller contribution from land-use changes (IPCC, 2001). Levels of CO₂ are predicted to rise further unless emissions are reduced substantially. The global mean surface temperature is predicted to rise between 2.6 and 5.3 °C by 2100 (Johns et al., 2003).

The rise in temperature caused by increased levels of CO₂ will also impact on trace gas concentrations and air quality. Generally, chemical reactions involved in the conversion of primary pollutants (such as, nitric oxide (NO), carbon monoxide (CO) and hydrocarbons) to secondary pollutants (for example, ozone (O₃) and nitric acid (HNO₃)) will proceed more quickly. However, a warmer climate means that water vapour concentrations will increase. Consequently, production of the hydroxyl radical (OH) will also increase via reaction of water vapour with energetically excited oxygen atoms, which in turn are formed from ozone photolysis, thereby reducing ozone levels (Johnson et al., 2001).

There are a large number of indirect effects of climate change on global ozone levels. Stratosphere–troposphere exchange (STE) is an important source of ozone for the troposphere, and may increase in a warmer climate (Collins et al., 2003). Emissions of methane from wetlands will increase (Gedney et al., 2004). Methane itself is a greenhouse gas, and oxidation of methane in the troposphere strongly controls global ozone levels (Wild and Prather, 2000). Emission of reactive hydrocarbons such as isoprene by vegetation may also increase in a warmer climate (Sanderson et al., 2003). These hydrocarbons play a key role in the production and loss of ozone (Wang and Shallcross, 2000). Convection may increase in a warmer climate, resulting in increased frequency of lightning and consequently more production of nitrogen oxides (Price et al., 1997). These latter species also play a key role in the production of ozone. There are also likely to be changes in large-scale meteorology, cloud cover and precipitation, all of which will change the transport of ozone and its precursors, as well as impacting on the chemical reactions (Stevenson et al., 2005).

There is an additional indirect impact of increasing levels of CO₂ on surface ozone levels, which has generally not been included in simulations of future trace gas concentrations. Many pollutants, such as ozone, nitric acid and nitrogen dioxide are removed from the atmosphere by a process called dry deposition. This process may be defined as the irreversible removal of trace gases at the surface in the absence of precipitation (Seinfeld and Pandis, 1998). CO₂ levels influence the size of small pores on the surface of leaves called stomata, which allow carbon

*Corresponding author.
e-mail: michael.sanderson@metoffice.gov.uk
DOI: 10.1111/j.1600-0889.2007.00277.x

dioxide for photosynthesis to enter the plant, and water to escape. Pollutants can be deposited to vegetation, to the branches, leaf surfaces (cuticle) and also to the interior of the leaf via the stomata. The size of the stomatal pores is controlled by many factors, such as the intensity of sunlight, soil moisture, and, as already mentioned, the level of carbon dioxide in the atmosphere. Plant growth generally increases with higher levels of CO₂, as most are limited by the availability of CO₂ (Taiz and Zeiger, 1991). However, increasing levels of CO₂ allow partial closure of the stomata, as they do not need to open as widely to allow sufficient CO₂ for photosynthesis to enter the leaf (IPCC, 2001). Consequently, the rate of removal of pollutants via dry deposition may also fall, and their surface concentrations could rise.

Stomatal conductance (g_s; m s⁻¹) may be related to the photosynthetic CO₂ assimilation rate (A; mol CO₂ m⁻² s⁻¹) using the following equation (Cox, 2001),

$$A = g_s(C_c - C_i)/1.6RT, \quad (1)$$

where C_c and C_i are the partial pressures of CO₂ in the ambient air and the inter-cellular spaces inside the leaf, respectively, R is ideal gas constant, T is the leaf temperature and the factor of 1.6 is the ratio of the diffusivities of water and carbon dioxide. Taiz and Zeiger (1991) have presented measured assimilation rates and calculated intercellular CO₂ partial pressures for a C₃ plant under a wide range of ambient CO₂ concentrations. Most species of natural vegetation and crops in Europe belong to the C₃ family. Using those data and eq. (1), the stomatal conductance was calculated to fall to 62% of its original value if the current level of CO₂ in the atmosphere was doubled. There are many other measurements illustrating the reduction in stomatal conductance under elevated CO₂ levels. For example, Bunce (2000) found that the stomatal conductance of wheat was reduced to between 33 and 80% of its original value under approximately doubled CO₂ conditions. Similar results for barley were found, with stomatal conductance falling to between 42 and 86% of its original value. Li et al. (2003) reported stomatal conductances that were 61 and 69% of their original values in May and October, respectively, for a species of oak when grown under doubled CO₂ levels. Herrick et al. (2004) examined the effect of elevated CO₂ levels on the stomatal conductance of a sweet-gum species (a common deciduous tree in parts of the USA). They found that the conductance was reduced to 72% of its original value when the CO₂ level was increased by 200 ppm. Bettarini et al. (1998) studied the effects of naturally emitted CO₂ in Italy on the surrounding vegetation. This emission results in double-ambient levels of CO₂. They found that the stomatal conductances fell to between 27 and 81% of their original values, depending on the particular species examined. All of these measurements show that increased levels of CO₂ significantly reduce stomatal conductance in a wide range of plant species.

In this paper, we present results from simulations investigating the effect of increasing CO₂ levels on stomatal conductance and surface concentrations of ozone, for both the present day and pre-

industrial periods. It should be noted that this effect is studied in isolation, to identify the sensitivity of modelled ozone levels to the stomatal conductance. In reality, many other factors will also play a role. In the following sections, the models and the simulations used are described. Next, the changes in stomatal conductance are discussed, followed by the changes in surface ozone levels. The possible impacts of changed meteorology are briefly described. Finally, the effect on modelled pre-industrial ozone levels is shown.

2. Model description

An atmosphere-only version (HadGAM1) of the Hadley Centre's climate model HadGEM1 (Johns et al., 2004) was coupled to the Lagrangian tropospheric chemistry model STOCHEM. In this study, HadGAM1 has a horizontal resolution of 3.75° × 2.5° and 38 vertical levels, extending to a height of 40 km above mean sea level. Climate data for the simulations (sea surface temperatures and sea ice extent) were taken from integrations of the previous Hadley Centre model HadCM3 which used levels of CO₂ and other radiatively active trace gases and aerosols appropriate for the year 2000 and the pre-industrial period (Johns et al., 2003).

The physiological processes of photosynthesis, respiration and transpiration for each of five Plant Functional Types (PFTs: broadleaf tree, needleleaf tree, C₃ grass, C₄ grass and shrub) are simulated by the MOSES land surface scheme (Essery et al., 2001) on the basis of the near-surface climate and atmospheric CO₂ concentrations. MOSES also incorporates a hydrology module, which calculates many other data, including soil moisture, run-off and surface heat fluxes.

The STOCHEM model has been described in detail elsewhere (Sanderson et al., 2003, and references therein). Briefly, the troposphere is divided into 100,000 air parcels of equal mass which are advected every 30 min using winds from the HadGAM1 model. Many other fields are passed from HadGAM1 to STOCHEM, including humidity, temperature, surface heat fluxes, convective mass fluxes and surface radiation fluxes. Each air parcel holds the concentrations of 80 chemical species, which react according to over 170 photolytic and chemical reactions with a 5 min time step. The resulting parcel concentrations are mapped onto the same horizontal grid as HadGAM1, but only 20 vertical levels, which extend to the same height as HadGAM1 (40 km). The coarser vertical grid is used to ensure sufficient air parcels are present in each level at each time step.

The version of STOCHEM used here has the same model of natural hydrocarbon emissions as described by Sanderson et al. (2003). Dry deposition fluxes of many trace gases, including ozone, nitrogen dioxide (NO₂), nitric acid (HNO₃) and hydrogen peroxide (H₂O₂) are calculated using a 'big leaf' model. A full description of this type of model is given by Seinfeld and Pandis (1998) and Smith et al. (2000), so only a brief summary is given here. In this approach, the dry deposition process is broken down into three steps: (1) an aerodynamic term, which

controls the transport of species through the boundary layer to a thin layer of air just above the surface, (2) transport through this thin layer, called the quasi-laminar layer and (3) uptake at the surface itself. Each step is treated as a resistance term, so that the overall deposition velocity may be calculated by combining these resistance terms (Seinfeld and Pandis, 1998). The deposition flux of a species is then simply calculated as the product of the dry deposition velocity and the surface trace gas concentration. Standard equations for the aerodynamic and quasi-laminar resistances were used (Seinfeld and Pandis, 1998), the former incorporating the vertical momentum and temperature profiles recommended by Dyer (1974).

The surface resistance term (which is generally referred to as R_c) is the most complicated, as it is calculated from many individual resistance terms representing the different surfaces that a trace gas may deposit to, including the leaf cuticles, soil underneath the vegetation and the interior of the leaf via the stomata (Seinfeld and Pandis, 1998; Smith et al., 2000). The individual terms used to calculate the overall surface resistance are illustrated in Fig. 1. Not all these terms will be required at

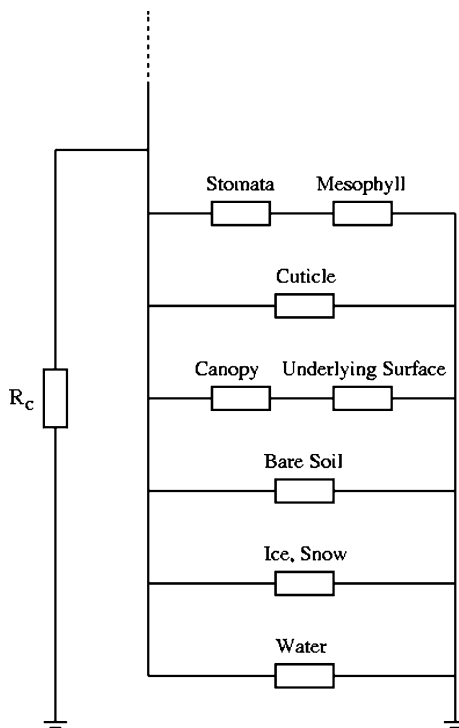


Fig. 1. Illustration of the individual terms used to calculate the overall surface resistance for dry deposition of pollutants (R_c). Not all the terms will be required at every surface location within the model. The term 'canopy' refers to the physical obstruction by the leaves of the plants to downward movement of air to reach the soil underneath. The resistance to deposition for this soil is the 'underlying surface'. The characteristics of this soil are likely to be very different to those of bare soils. For non-vegetated land, $R_c = R(\text{bare soil})$. For water, $R_c = R(\text{water})$, and for areas covered by ice or snow, $R_c = R(\text{ice, snow})$.

each surface location in the model. For vegetated areas, during the hours of daylight, the stomata will be open, and deposition of pollutants to the interior of the plant via the stomata can occur. This route represents the major daytime sink for some pollutants, particularly ozone. During the night, the stomata will be closed, and deposition to the cuticles and underlying soil will be the major loss routes. All of these different deposition routes at the surface are therefore important, and are considered at all times. For example, van Pul and Jacobs (1994) studied ozone deposition over a maize field, and showed that deposition to the underlying soils accounted for between 0 and 65% of the total deposition flux, depending on the soil moisture. Ozone is known to cause damage to plants if it is deposited to the interior of leaves (Crous et al., 2006); however, any damage and subsequent impact on photosynthesis and stomatal conductance is not considered in the present work.

The mesophyll resistance term in Fig. 1 (which represents deposition to the interior of the leaf) is assumed to be small compared to the stomatal resistance term, and is ignored, except for the deposition of NO_2 , where it is set to 50% of the stomatal resistance term (Ganzeveld and Lelieveld, 1995). The term 'canopy' refers to an in-canopy aerodynamic resistance, which represents the physical resistance to the movement of air through the foliage of the plant to reach the underlying surface (van Pul and Jacobs, 1994). The underlying surface refers to the resistance to deposition of the soil underneath the vegetation. This term is given a fixed value for each depositing species. For non-vegetated land, the surface resistance is equal to the bare soil resistance term in Fig. 1, i.e., $R_c = R(\text{bare soil})$. For water, $R_c = R(\text{water})$ and for areas covered by ice or snow, $R_c = R(\text{ice, snow})$. Values for the various resistance terms in Fig. 1 were assigned using published values (Ganzeveld and Lelieveld, 1995).

Stomatal conductance is calculated within the MOSES land surface scheme. Gross photosynthesis rates are calculated using the models of Collatz et al. (1991, 1992), which, combined with eq. (1) and the closure equation of Jacobs (1994), are then used to calculate the stomatal conductance. Further details are given by Cox (2001). It should be noted that the different equation linking stomatal conductance and photosynthetic assimilation rates cited by Collatz et al. (1991) is not used in MOSES.

3. Model simulations

Five model simulations were used to assess the effect of increasing CO_2 levels on stomatal conductance and surface trace gas concentrations. They are summarized in Table 1. First, a control simulation was run, which used present-day CO_2 levels and climate information for the year 2000. The meteorology generated by HadGAM1 in each year of the simulation will be different, but still appropriate for the beginning of the 21st century. The second simulation involved the calculation of two stomatal conductances, using current and doubled levels of CO_2 . The

Table 1. Summary of model simulations. $1 \times \text{CO}_2$ corresponds to present-day levels (369 ppm; IPCC, 2001). 280 ppm CO_2 is used for the pre-industrial period. $2 \times \text{CO}_2$ refers to double present-day levels.

Stomatal conductance used:

Simulation	STOCHEM	GCM
1	$1 \times \text{CO}_2$	$1 \times \text{CO}_2$
2	$2 \times \text{CO}_2$	$1 \times \text{CO}_2$
3	$2 \times \text{CO}_2$	$2 \times \text{CO}_2$
4	280 ppm	280 ppm
5	$1 \times \text{CO}_2$	280 ppm

stomatal conductances calculated using doubled CO_2 levels were only passed to STOCHEM for use in the dry deposition module. The underlying GCM used the conductances calculated with current CO_2 levels. In the third simulation, the stomatal conductance was calculated using doubled CO_2 levels only, and was used in both the GCM and STOCHEM. In this third case, the water vapour concentration at the surface will change, owing to reduced transpiration, and hence change cloud amount, precipitation, run-off and meteorology (Gedney et al., 2006). In simulations 1–3, anthropogenic emissions of primary pollutants were taken from the International Institute for Applied Systems Analysis (IIASA) estimates for the year 2000 (Dentener et al., 2005). The final two simulations used a climatology and emissions suitable for the pre-industrial period (Gauss et al., 2006). Simulation 4 used 280 ppm CO_2 , appropriate for the pre-industrial period (IPCC, 2001). Simulation 5 is similar to simulation 2, in that two stomatal conductances were calculated, but using 280 ppm and 369 ppm CO_2 (for the year 2000). The stomatal conductances calculated using 369 ppm CO_2 were only passed to STOCHEM.

In all simulations, to save time spinning up the model, and to help constrain the results, global methane mixing ratios were specified across the model domain, using results from previous model integrations using the same emission scenarios. This approach has been used recently for multi-model ensemble predictions of past, current and future tropospheric ozone levels (Gauss et al., 2006; Stevenson et al., 2006). Each model simulation lasted for 5 years and 4 months. The first 3 months are used to spin up the model and are excluded from the analysis. During this period, the levels of short-lived trace gases, such as ozone, NO_x and carbon monoxide will adjust from their prescribed initial concentrations to those determined by the particular chemistry and meteorology used.

4. Results

4.1. Validation of modelled ozone levels

The ozone levels in the current version of STOCHEM have been validated recently (Gauss et al., 2006; Stevenson et al., 2006). However, the STOCHEM simulations used in these papers em-

Table 2. Summary of ozone budgets, as defined by Stevenson et al. (2006). Chemical production (P), chemical loss (L), dry deposition (D) and inferred stratospheric input (S; defined as L + D – P) have units of $\text{Tg O}_3 \text{ yr}^{-1}$. The tropospheric burden (B) and ozone lifetime (τ_{O_3}) are also given. The ‘Mean Model’ row shows the average values over all models from Stevenson et al. (2006), as given in their ‘Table 5’. The ‘Original’ row gives the results from STOCHEM-HadGAM when the simpler dry deposition scheme was used, also listed in the study by Stevenson et al. (2006). All the data shown below are averaged over 5 years.

	P	L	D	S	B (Tg O_3)	τ_{O_3} (days)
Mean model	5110	4668	1003	552	344	22.3
Original	5114	3757	1507	151	293	20.3
Simulation 1	5336	4413	1055	131	274	18.1

ployed a simple dry deposition scheme, which used fixed surface resistance values for land, sea and ice. To assess the impact of the new dry deposition scheme, the global ozone budget from simulation 1 was examined, using the production (P), loss (L) dry deposition (D), inferred stratospheric input (S, calculated as L + D – P), tropospheric burden (B) and lifetime (τ , defined as B / (L + D)) terms. The values of each of these terms are compared with the values listed by Stevenson et al. (2006) in Table 2, which also includes the terms for STOCHEM-HadGAM1 calculated when the simpler dry deposition scheme was used. Simulation 1 is identical to simulation ‘S1’ described by Stevenson et al. (2006), apart from the dry deposition scheme used. In the present work, the ozone budget terms are ($\text{Tg O}_3 \text{ yr}^{-1}$): P = 5336, L = 4413 and D = 1055 for simulation 1. Overall, the values of the three terms P, L and D calculated from simulation 1 agree well with the mean model results given by Stevenson et al. (2006), and are an improvement over the values calculated when the simple dry deposition scheme was used. The inferred stratospheric input term in simulation 1 is 131 $\text{Tg O}_3 \text{ yr}^{-1}$, which is slightly worse than the previous STOCHEM value of 151 $\text{Tg O}_3 \text{ yr}^{-1}$ (Stevenson et al., 2006). However, the stratospheric ozone flux calculated dynamically is 317 $\text{Tg O}_3 \text{ yr}^{-1}$, which is still low but nearer the mean model value.

4.2. Changes in stomatal conductance

The changes in stomatal conductance between simulations 1 and 2, averaged over all PFTs, are shown in Fig. 2. A negative value indicates that the stomatal conductance is smaller in simulation 2 (which has doubled CO_2 levels) than simulation 1. In all areas of the globe, the changes are negative, indicating that the stomatal conductance is smaller when doubled CO_2 levels are used. The conductance is generally 0.5–2.0 mm s^{-1} smaller over large parts of the landmasses in all four seasons, with a few larger differences in spring (MAM) and summer (JJA). This change represents a significant decrease in stomatal conductance. Not surprisingly, there is no change over much of the Northern Hemisphere in winter (DJF) when plants are light-limited rather than

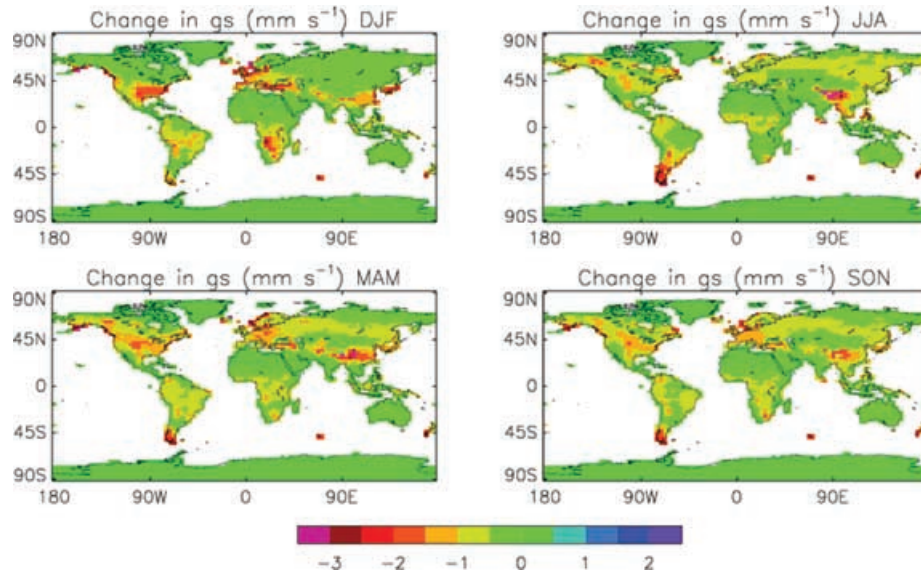


Fig. 2. Changes in seasonal mean stomatal conductances (g_s ; mm s^{-1}) for winter (DJF), spring (MAM), summer (JJA) and autumn (SON) when the CO_2 value is doubled. A negative value indicates that the stomatal conductances are smaller in simulation 2 than simulation 1. See Table 1 and text for more details.

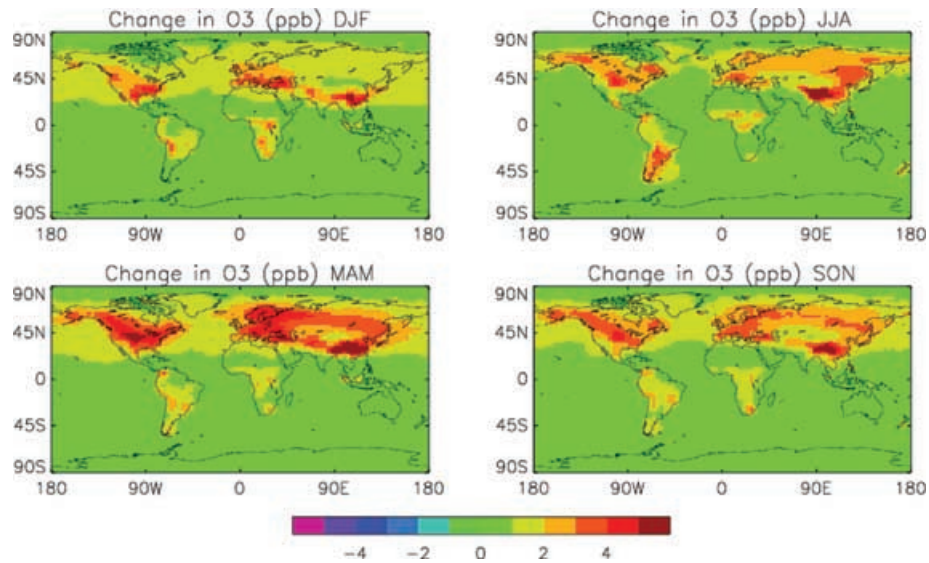


Fig. 3. Changes in seasonal mean surface ozone concentrations (ppb) for winter (DJF), spring (MAM), summer (JJA) and autumn (SON) when the stomatal conductance calculated using a doubled CO_2 value is passed to the chemistry model only. A positive value indicates that the ozone levels are larger in simulation 2 than simulation 1. See Table 1 and text for more details.

CO_2 -limited. Changes of slightly smaller magnitudes are seen over South America and Africa, although in the latter case the changes in autumn (MAM) and winter (JJA) are very small, owing to the dry soils during this period. No significant change in stomatal conductance is modelled over Australia.

4.3. Differences in surface trace gas concentrations

The changes in surface ozone levels between simulations 1 and 2 over Europe in the four seasons are shown in Fig. 3. These

changes demonstrate the effect of reduced stomatal conductances (and hence smaller dry deposition fluxes) on surface ozone levels caused by doubled CO_2 concentrations, but with no change in meteorology. In all four seasons, the ozone levels are larger, by up to 8 ppb, although a change of 3–4 ppb is seen over the majority of the northern hemisphere land masses. These changes correspond to ozone increases of between 5 and 20%, which is large. The standard deviations of the ozone changes at each surface point in the model were also calculated. These were almost always much smaller than the changes in ozone. The exception

was the ozone increases projected for the autumn (SON), where the standard deviations were approximately half the size of the change itself. In no case was the standard deviation larger than the change in ozone levels, showing that these increases are significant. The sizes of the ozone increases are larger than the year-to-year variability.

A comparison of Fig. 2 and 3 shows that areas with reduced stomatal conductance, and areas with increased surface ozone levels, are in approximately the same place. The ozone increases tend to occupy a larger area. Ozone has a lifetime of about 18 d in the present work (Table 2), which is long enough for it to be transported away from the regions with reduced stomatal conductance. This result demonstrates that deposition to plants via the stomata has a significant impact on surface ozone levels.

The distributions of the changes in surface ozone levels are very different in each season. The largest changes in the northern hemisphere are seen in the spring (MAM), when most of the vegetation and crops are growing, and the stomata are fully open. In this case, the surface ozone levels are 3–6 ppb larger over most of Europe and North America. Changes of similar magnitudes are also seen in the autumn (SON). The smallest impact of the doubled CO₂ levels on stomatal conductance is seen in the summer (JJA). The deposition flux of ozone via the stomata is smallest during this period, as plants restrict the opening of the stomata to conserve water.

In the Southern Hemisphere, smaller changes in surface ozone levels are seen in all four seasons. Over South America, ozone levels are up to 6 ppb larger in the Southern Hemisphere winter (JJA) and spring (SON), with increases between 1 and 2 ppb in the other seasons. Smaller changes are seen over Africa, between 1 and 3 ppb in all seasons except the winter (DJF) when slightly larger increases of 2–3 ppb are modelled.

Changes in the surface levels of other important pollutants, such as nitrogen oxides (NO_x; NO + NO₂) and peroxyacetyl nitrate (PAN) were also examined. Both of these species play an important role in ozone formation, and are also dry deposited. However, there was essentially no change in the surface levels of NO_x and PAN. Dry deposition is a major loss process for ozone, but is less important for other species. In the present work, the change in the dry deposition fluxes of NO_x and PAN is clearly too small to impact on their modelled concentrations. The reduced stomatal conductance therefore appears to have little effect on the concentrations of NO_x and other species containing oxidised nitrogen.

4.4. Changes in meteorology and surface trace gas concentrations

In simulation 3, doubled CO₂ levels were used to calculate stomatal conductances for the land surface exchange of water vapour as well as ozone. The rate of transpiration of water from plants, and hence surface water vapour concentrations, will be reduced, with consequent changes in cloud cover, surface temperature and

meteorology. A comparison of results from simulations 1 and 3 will show the difference in surface concentrations of trace gases caused by both meteorology and dry deposition changes. The changes in stomatal conductance between simulations 1 and 3 are different to those modelled in simulations 1 and 2, owing to increased levels of soil moisture. The patterns of the changes are broadly similar to those shown in Fig. 1, but the magnitudes are smaller.

The changes in surface ozone values between simulations 1 and 3 are very different to those in Fig. 3 (data not shown). There are many areas where the ozone levels in simulation 3 are smaller than those in simulation 1, as well as areas with larger ozone levels. These changes will be caused by differences in humidity and meteorology as discussed previously, as well as reduced dry deposition fluxes.

4.5. Impact on modelled pre-industrial ozone levels

Ozone levels in pre-industrial times (nominally 1850) are known to be much smaller than present-day values. The earliest measurements of ozone were made in the second half of the 19th century. Modern analysis of these data indicate that, at least over parts of France, ozone levels lay between 7 and 10 ppb in Montsouris, Paris, for the period 1876–1886 (Volz and Kley, 1988), and around 10 ppb at the Pic du Midi in the south-west for the same period (Marencio et al., 1994). Measured ozone levels in many other areas of the globe did not exceed 16 ppb (Hauglustaine and Brasseur, 2001). However, with the possible exception of the Montsouris measurements, for which a different technique was used (Volz and Kley, 1988), the ozone measurements made during the second half of the 19th century have large errors (± 5 ppb), are difficult to quantify, and may be unreliable (Hauglustaine and Brasseur, 2001). Many global models tend to predict larger ozone levels than those suggested by these early measurements. There are a number of possible reasons, particularly incorrect biomass burning, lightning and soil NO_x emissions. Hauglustaine and Brasseur (2001) showed that their modelled pre-industrial ozone levels were very sensitive to these three emission sources. The impact of CO₂ changes on the ozone deposition flux via the stomata has not been considered in previous studies of pre-industrial ozone levels.

Two additional simulations (4 and 5 in Table 1) were performed, to examine just the effect of increasing CO₂ levels on modelled pre-industrial ozone levels. In simulation 4, surface ozone levels of ozone over Montsouris lie between 12 and 16 ppb, with an annual average of 14 ppb. The annual average value is 1.4–2.0 times larger than the measured ozone levels. The change in annual mean surface ozone levels over Europe (simulation 4 minus simulation 5) owing to smaller CO₂ levels (and hence increased ozone deposition fluxes) are shown in Fig. 4. It can be seen that the ozone levels are a maximum of 1.5 ppb smaller if a CO₂ level of 280 ppm is used, instead of 369 ppm. The annual average ozone level over Paris is only about 1 ppb

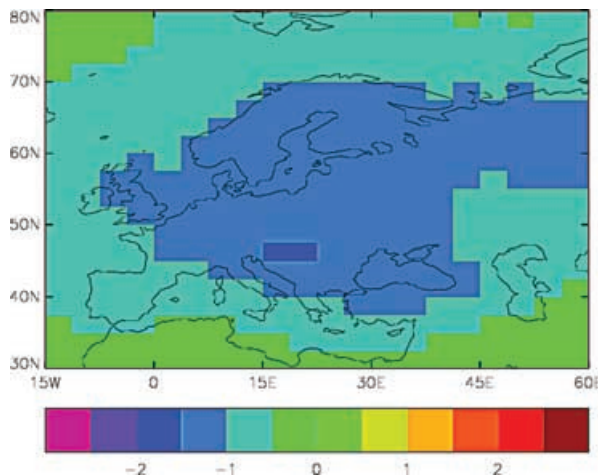


Fig. 4. Changes in annual mean surface ozone concentrations (ppb) for the pre-industrial period when the stomatal conductance calculated using 369 ppm CO₂ is passed to the chemistry model only. A negative value indicates that the ozone levels are smaller in simulation 4 than simulation 5. See Table 1 and text for more details.

smaller. Hence, changes in stomatal conductance due to different CO₂ levels only have a small impact on modelled ozone levels during the pre-industrial period.

5. Discussion and conclusions

In this study, we have used a coupled chemistry-climate model to investigate the impact of increasing CO₂ levels on surface ozone concentrations. CO₂ levels have a large influence on stomatal conductance, which controls the dry deposition flux of ozone and other pollutants. As the CO₂ levels continue to rise, the stomata will not open as widely, which has the effect of reducing the dry deposition flux of ozone, and hence its surface concentrations will rise. Ozone levels are also rising, owing to increases in emissions of precursor gases, such as NO_x and hydrocarbons. If the dry deposition flux of ozone is reduced, the future surface ozone values may be even higher. Previous studies of future air quality have not included the indirect impact of CO₂ increases via stomatal conductance.

In the present work, experiments to investigate the effects of doubled CO₂ concentrations on stomatal conductance and hence ozone dry deposition fluxes and surface ozone levels, while not changing the meteorology, were performed. The results showed that surface ozone levels over large parts of the Northern Hemisphere rose by between 2 and 8 ppb, or 5–20%, throughout the year compared to a model simulation with present-day CO₂ concentrations. No change in the surface concentrations of NO_x or PAN was found.

An additional experiment included the effects of doubled CO₂ on the land surface exchange of water vapour, as well as the deposition of trace gases. The changes in ozone and other pollutants

were very different to those modelled when the only effect was on the ozone dry deposition flux, with both positive and negative changes in the surface concentrations.

The possible impact of increasing CO₂ levels on modelled pre-industrial levels of ozone was also investigated. Previous work has shown that ozone levels are highly sensitive to biomass burning emissions, soil NO_x emissions and production of NO_x by lightning (Hauglustaine and Brasseur, 2001). Changing the stomatal conductance by increasing the CO₂ level from 280 ppm to 369 ppm only reduced the modelled surface ozone values over much of Europe by about 1 ppb. The precursor emissions identified by Hauglustaine and Brasseur (2001) are likely to be of greater importance in controlling modelled ozone levels for this period.

The limitations of this work should be emphasized. The ozone changes described in this study only consider changes in stomatal conductance caused by changes in CO₂ levels. This allows the effect of dry deposition changes alone on surface ozone values to be identified. For the present day, ozone levels were larger over most of the landmasses if the CO₂ level was doubled. However, other factors are likely to have significant impacts as well. In reality, any changes in stomatal conductance will also affect water vapour, cloud formation, surface temperatures and hence the surface meteorology. A simulation including these impacts showed that the modelled ozone changes were very different, and included both positive and negative changes. The exact location and magnitude of these changes will be very dependent on the location and size of emissions of pollutants. This means that results from simulations including the stomatal impact on future ozone predictions will need careful interpretation. Simulations using a variety of emission scenarios will be required.

The results presented in this study should only be regarded as an indication of possible impacts of changes in stomatal conductance on modelled surface ozone levels. Overall, the results indicate that increasing levels of carbon dioxide result in larger surface ozone levels via changes in stomatal conductance. This interaction should be included in simulations of future ozone concentrations.

6. Acknowledgments

The authors would like to thank the Met Office Government Meteorological Research Programme, and the U.K. Department for Environment, Food and Rural Affairs (Air Quality Division) for financial assistance under contracts PECD 7/12/37 and CPEA7 respectively.

References

- Bettarini, I., Vaccari, F. P. and Miglietta, F. 1998. Elevated CO₂ concentrations and stomatal density: observations from 17 plant species growing in a CO₂ spring in central Italy. *Global Change Biol.* **4**, 17–22.

- Bunce, J. A. 2000. Responses of stomatal conductance to light, humidity and temperature in winter wheat and barley grown at three concentrations of carbon dioxide in the field. *Global Change Biol.*, **6** 371–382.
- Collatz, G. J., Ball, J. T., Grivet, C. and Berry, J. A. 1991. Physiological and environmental regulation of stomatal conductance, photosynthesis and transpiration: A model that includes a laminar boundary layer. *Agric. For. Meteorol.* **54**, 107–136.
- Collatz, G. J., Ribas-Carbo, M. and Berry, J. A. 1992. A coupled photosynthesis-stomatal conductance model for leaves of C₄ plants. *Aus. J. Plant Physiol.* **54**, 107–136.
- Collins, W. J., Derwent, R. G., Garnier, B., Johnson, C. E., Sanderson, M. G. and co-authors. 2003. Effect of stratosphere-troposphere exchange on the future tropospheric ozone trend. *J. Geophys. Res.* **108**, 8528, doi:10.1029/2002JD002617.
- Cox, P. M. 2001. Description of the TRIFFID global dynamic vegetation model, *Hadley Centre Technical Note No.24*, Met Office, Exeter, U.K. <http://www.metoffice.gov.uk/research/hadleycentre/pubs/HCTN>
- Crous, K. Y., Vandermeiren, K. and Ceulemans, R. 2006. Physiological responses to cumulative ozone uptake in two white clover (*Trifolium repens L. cv. Regal*) clones with different ozone sensitivity. *Environ. Experiment. Bot.* **58**, 169–179.
- Dentener, F. D., Stevenson, D. S., Cofala, J., Mechler, R., Amann, M. and co-authors. 2005. The impact of air pollutant and methane emissions controls on tropospheric ozone and radiative forcing: CTM calculations for the period 1990–2030. *Atmos. Chem. Phys.* **5**, 1731–1755.
- Dyer, A. J. 1974. A review of flux-profile relationships. *Bound. Layer Meteorol.* **7**, 363–372.
- Essery, R., Best, M. and Cox, P. 2001. MOSES 2.2 Technical Documentation, *Hadley Centre Technical Note No.30*, Met Office, Exeter, U.K. <http://www.metoffice.gov.uk/research/hadleycentre/pubs/HCTN>
- Ganzeveld, L. and Lelieveld, J. 1995. Dry deposition parametrization in a chemistry general circulation model and its influence on the distribution of reactive trace gases. *J. Geophys. Res.* **100**, 20999–21012.
- Gauss, M., Myhre, G., Isaksen, I. S. A., Grewe, V., Pitari, G. and co-authors. 2006. Radiative forcing since pre-industrial times due to ozone change in the troposphere and the lower stratosphere. *Atmos. Chem. Phys.* **6**, 575–599.
- Gedney, N., Cox, P. M. and Huntingford, C. 2004. Climate feedback from wetland methane emissions. *Geophys. Res. Lett.* **31**, L20503, doi:10.1029/2004GL020919.
- Gedney, N., Cox, P. M., Betts, R. A., Boucher, O., Huntingford, C. and co-authors. 2006. Detection of a direct carbon dioxide effect in continental river runoff records. *Nature* **439**, 835–838.
- Hauglustaine, D. A. and Brasseur, G. P. 2001. Evolution of tropospheric ozone under anthropogenic activities and associated radiative forcing of climate. *J. Geophys. Res.* **106**, 32377–32360.
- Herrick, J. D., Maherli, H. and Thomas, R. B. 2004. Reduced stomatal conductance in sweetgum (*Liquidambar styraciflua*) sustained over long term CO₂ enrichment. *New Phytol.* **162**, 387–396.
- IPCC 2001. *Climate Change 2001: The scientific basis*. Contribution of working group I to the third assessment report of the intergovernmental panel on climate change (eds. J. T. Houghton, Y. Ding, D. J. Griggs, M. Noguer, P. J. van der Linden, X. Dai, K. Maskell and C. A. Johnson), Cambridge University Press, Cambridge.
- Jacobs, C. 1994. Direct impacts of atmospheric CO₂ enrichment on regional transpiration. Ph.D. thesis, Wageningen Agricultural University, The Netherlands.
- Johns, T. C., Gregory, J. M., Ingram, W. J., Johnson, C. E., Jones, A., and co-authors. 2003. Anthropogenic climate change for 1860 to 2100 simulated with the HadCM3 model under updated emission scenarios. *Clim. Dyn.* **20**, 583–612.
- Johns, T., Durman, C., Banks, H., Roberts, M., McLaren, A., and co-authors. 2004. HadGEM1 - Model description and analysis of preliminary experiments for the IPCC Fourth Assessment Report, *Hadley Centre Technical Note No. 55*, Met Office, Exeter, U.K. <http://www.metoffice.gov.uk/research/hadleycentre/pubs/HCTN>
- Johnson, C. E., Stevenson, D. S., Collins, W. J. and Derwent, R. G. 2001. Role of climate feedback on methane and ozone studied with a coupled ocean-atmosphere-chemistry model. *Geophys. Res. Lett.* **28**, 1723–1726.
- Marenci, A., Gouget, H., Nédélec, P., Pagès, J.-P. and Kärcher, F. 1994. Evidence of a long-term increase in tropospheric ozone from Pic du Midi data series: Consequences – positive radiative forcing. *J. Geophys. Res.* **99**, 16617–16632.
- Price, C., Penner, J. and Prather, M. 1997. NO_x from lightning 1. Global distribution based on lightning physics. *J. Geophys. Res.* **102**, 5929–5941.
- van Pul, W. A. J. and Jacobs, A. F. G. 1994. The conductance of a maize crop and the underlying soil to ozone under various environmental conditions. *Bound. Layer Meteorol.* **69**, 83–99.
- Sanderson, M. G., Jones, C. D., Collins, W. J., Johnson, C. E. and Derwent, R. G. 2003. Effect of climate change on isoprene emissions and surface ozone levels. *Geophys. Res. Lett.* **30**, 1936, doi:10.1029/GL017642.
- Seinfeld, J. H. and Pandis, S. N. 1998. *Atmospheric Chemistry and Physics*, John Wiley and Sons, New York.
- Smith, R. I., Fowler, D., Sutton, M. A., Flechard, C. and Coyle, M. 2000. Regional estimation of pollutant gas dry deposition in the UK: model description, sensitivity analyses and outputs. *Atmos. Environ.* **34**, 3757–3777.
- Stevenson, D. S., Doherty, R. M., Sanderson, M. G., Johnson, C. E., Collins, W. J. and co-authors. 2005. Impacts of climate change and variability on tropospheric ozone and its precursors. *Farad. Discuss.* **130**, 41–57, doi:10.1039/b417412g.
- Stevenson, D. S., Dentener, F. J., Schultz, M. G., Ellingsen, K., Van Noije, T. P. C., and co-authors. 2006. Multi-model ensemble simulations of present day and near future tropospheric ozone. *J. Geophys. Res.* **111**, D08301, doi:10.1029/2005JD006338.
- Taiz, L. and Zeiger, E. 1991. *Plant Physiology*, Benjamin/Cummings Publishing, Redwood City, California.
- Volz, A. and Kley, D. 1988. Evaluation of the Montsouris series of ozone measurements made in the nineteenth century. *Nature* **332**, 240–242.
- Wang, K.-Y. and Shallcross, D. E. 2000. Modelling terrestrial biogenic isoprene fluxes and their potential impact on global chemical species using a coupled LSM-CTM model. *Atmos. Environ.* **34**, 2909–2925.
- Wild, O. and Prather, M. J. 2000. Excitation of the primary tropospheric chemical mode in a global three-dimensional model. *J. Geophys. Res.* **105**, 24647–24660.